Letters

A Bidirectional MVDC Solid-State Circuit Breaker Based on Mixture Device

Jin Zhu, *Member, IEEE*, Qingpeng Zeng, *Graduate Student Member, IEEE*, Xu Yang, Mi Zhou, and Tongzhen Wei

***Abstract*—The mixture unidirectional solid-state circuit breaker (SSCB) based on transistor-based devices [i.e., IGBT-based line commutation switch (LCS)] and the thyristor-based devices can combine their respective advantages, however, the conduction loss and cost may increase significantly when expanding to a bidirectional topology because the number of IGBTs had to be doubled with the expansion of unidirectional LCS structure to bidirectional LCS structure composed of two groups of IGBTs in reverse series. In this letter, a full-bridge mixture bidirectional SSCB (FB-MSSCB) requiring only one unidirectional LCS is proposed, the required number of IGBTs can be reduced by at least half compared with other mixture bidirectional SSCB topologies in the same voltage and current level applications. As a result, the FB-MSSCB has advantages of more economic design and higher efficiency, the conduction loss can be reduced by at least 23.3% in 10 kV MVdc system, while retaining other advantages of mixture bidirectional SSCB, such as the ability to actively interrupt bidirectional fault currents, without introducing additional thyristors, charging power supply, and charging strategy. The working principles and designing guidelines is presented in detail. The feasibility and effectiveness are verified by experiment results and comparative analysis.**

***Index Terms*—Bidirectional circuit breaker, mixture device, system protection, thyristor.**

I. Introduction

THE voltage-source-converter (VSC) based direct current (dc) power systems has been developed increasingly in renewable energy connections because of its significant advantages such as flexible control, high efficiency, less complex system, and higher stability [1]. However, fault blocking problems still prevent further application of this technology to widespread use due to the high fault current rising rate and the absence of natural zero-crossing point.

Manuscript received February 28, 2022; revised March 28, 2022 and April 20, 2022; accepted April 24, 2022. Date of publication May 3, 2022; date of current version June 24, 2022. This work was supported in part by the National Natural Science Foundation of China under Grant 51607171 and in part by the Institute of Electrical Engineering, CAS under Grants E155610301 and E155610201. *(Corresponding author: Qingpeng Zeng.)*

The authors are with the Institute of Electrical Engineering, Chinese Academy of Sciences, Beijing 100190, China (e-mail: zhujin@mail.iee.ac.cn; zengqingpeng19@mail.iee.ac.cn; yx_auto@whut.edu.cn; zhoumi@sics.ac.cn; tzwei@mail.iee.ac.cn).

Color versions of one or more figures in this article are available at https://doi.org/10.1109/TPEL.2022.3171805.

Digital Object Identifier 10.1109/TPEL.2022.3171805

Dc circuit breakers (dcCBs) play a vital role in isolating the fault area and maintaining normal operations of nonfault areas in dc power system. Various dc circuit breaker solutions have been proposed and can be classified into three main groups: mechanical dcCBs (MCBs), hybrid dcCBs (HCBs), solid-state dcCBs (SSCBs). The traditional MCB suffers from slow operation speed and high maintenance cost due to the arc problem at the mechanical contacts. The HCB is considered as an acceptable solution and has been applied in many VSC-HVdc practical projects [2]. The response time is significantly improved compared with MCB, but still not fast enough when it comes to dc microgrid and dc distribution system with lower rated voltage, because of the shorter time constants and higher prospective currents [3], [4]. In addition, mechanical ultrafast disconnector increases the weight, volume, and investment. Solid-state circuit breakers (SSCBs) are gaining more attention in the low voltage dc (LVdc) system and the medium voltage dc (MVdc) system in recent years to address these challenges. The work in [5] illustrates a full picture of current development of SSCB including power semiconductor technologies, circuit topology, voltage clamping, and gate driver. Different types of power semiconductor devices have been applied in solid-state switches. IGBT switches can be a reliable and efficient way in designing SSCBs [6], [7], but in bidirectional scenario, reverse series connection is required, and the loss will increase significantly, which needs to be further optimized. The solutions based on wide-band gap semiconductor have also been proposed (e.g., SiC JFET-based SSCB and GaN based SSCB) and show advantages of smaller conduction losses and shorter interruption time, however, the high device cost need to be overcome before widely used in dcCB [8], especially in MVdc.

As a semiconductor device with the lower loss and cost in MVdc system, thyristor is gaining more interest in dc system protection. However, as the thyristor is a half-controlled device, making it turned OFF reliably is a challenging task. Integrated gate-commutated thyristors (IGCTs) can be turned OFF actively by commutate the current from the cathode to the gate and forces the device to exit latch-up mode [9], however, the specially designed gate driver significantly increases costs and volume. Another way to turn OFF the thyristors is using additional external circuits to help the thyristors to interrupt the current. Additional capacitor is used to reverse-bias the thyristor in [10]. However, the additional charging power supply and charging

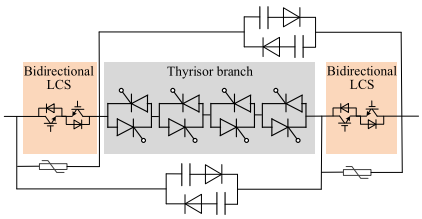

Fig. 1. Bidirectional structure of SSCB based on mixture device in [20].

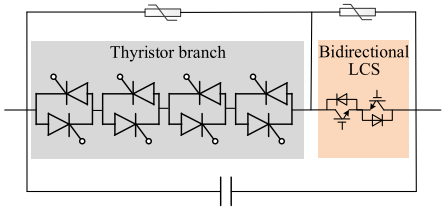

Fig. 2. Bidirectional structure of SSCB based on mixture device in [19].

TABLE I
COMPARISON OF CONDUCTION LOSS BETWEEN UNIDIRECTIONAL TOPOLOGY AND BIDIRECTIONAL TOPOLOGY IN [19]

	unidirectional topology	bidirectional topology
Conduction loss of Thyristor branch	5 kW	5 kW
Conduction loss of LCS	2.4 kW	4.65 kW
Total conduction loss	7.4 kW	9.65 kW

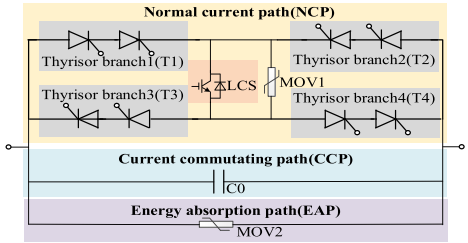

Fig. 3. Basic structure of the proposed bidirectional mixture SSCB.

control system will significantly increases the investment and complexity of the system. The solutions proposed in [11]–[13] can charge their commutating capacitor through dc sources, but the topologies and control strategies are too complicated to achieve compact integration and intelligent control. The Z-source, Γ-source, and T-source based solutions with simpler topology and simpler control strategy are used to generate the required reverse voltage on thyristor during the turn-OFF process [14]–[18]. However, those solutions can only be passively turned-OFF in the condition of the high current rising rate and not applicable to high resistance faults.

Mixing different types of semiconductors is now considered as an effective approach to achieve more cost-effective topologies, the topologies combing many thyristors with a few IGBTs-in-series is proposed in [19] and [20]. The required turn-OFF condition of thyristor can be generated by controlling IGBT to turn OFF, thus, can combine the low-loss and low-cost characteristics of thyristor and the active turn-OFF ability of IGBT in unidirectional topology. However, in bidirectional topologies, the number of IGBTs in the normal current path (NCP) will be doubled, because a bidirectional line commutation switch (LCS) composed of two groups of IGBTs in reverse series is needed, as shown in Figs. 1 and 2, which leads to significantly increased conduction loss in MVdc system, and more complex circuit structure.

In order to overcome the problems mentioned previously, a novel full-bridge solid-state circuit breaker based on mixture device (FB-MSSCB) is proposed, which is suitable for bidirectional protection of MVdc and HVdc systems. The main advantage of FB-MSSCB is that it can realize bidirectional fault blocking by requiring only one unidirectional LCS. Hence, the FB-MSSCB has advantages of higher efficiency, lower cost, and more compact design compared with other mixture device based SSCB, while retaining other advantages, such as the ability to actively interrupt fault currents, without introducing additional thyristors, charging power supply, and charging strategy.

II. PROPOSED TOPOLOGY

A. Basic Structure

Figs. 1 and 2 are the mixture device based bidirectional SSCB proposed in [19] and [20]. The number of IGBTs in the bidirectional topology will be doubled compared with the corresponding unidirectional topology, and the normal current flow through all IGBTs, which results in doubling the conduction loss caused by IGBT. Therefore, the cost and conduction loss of the whole bidirectional SSCB increases significantly.

Take 10 kV–1 kA MVdc system for example, eight 5.2 kV thyristor(T1451N) form the thyristor branch and two 4.5 kV IGBT(5SNA1200G452300) form the bidirectional LCS. The comparison of conduction loss between unidirectional topology and bidirectional topology in [19] is shown in Table I.

Obviously, compared with unidirectional LCS, the loss of bidirectional LCS will increase significantly. Therefore, the conduction loss of the whole SSCB will increased by at least 23.3%. Because the loss of bidirectional LCS part accounts for a large proportion, compared with the loss caused by current flowing through four thyristors of thyristor branch.

Fig. 3 shows the FB-MSSCB topology proposed in this letter. Same as other SSCB topologies, the basic structure of the proposed FB-MSSCB in this letter can be divided into three paths: 1) NCP, 2) current commutating path (CCP), and 3) energy absorption path (EAP). Inspired by classical symmetrical bridge topology, as shown in Fig. 4(a), a novel NCP circuit topology is proposed. But it is significantly different from the traditional bridge structure topology, as shown in Fig. 4(b). In the traditional symmetrical bridge topology, the voltage between "a" and "b" is equal to the system voltage, whether in symmetrical bridge converter or symmetrical bridge circuit breaker. However, the topology and control characteristics of the novel topology proposed in this letter make the voltage between "a" and "b" equal to only a small part of the system voltage.

Only one IGBT is required whether in the forward current path or the reverse current path, while the number of SCRs required

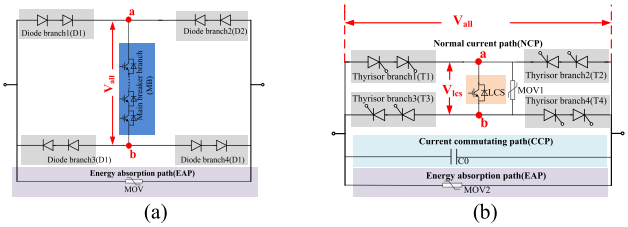

Fig. 4. Difference between the topology proposed in this letter and the traditional symmetric full bridge topology. (a) Traditional symmetrical bridge structure for SSCB. (b) Proposed novel FB-MSSCB topology.

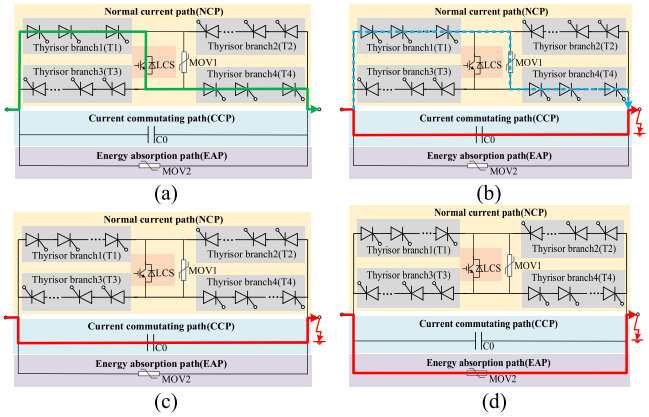

Fig. 5. Dc fault blocking principle. (a) Normal state of the system. (b) Step 1 of the principle. (c) Step 2 of the principle. (d) Step 3 of the principle.

is the same as the solutions in [19] and [20] (2 thyristors in each branch, eight thyristors in total for 10 kV MVdc SSCB). Hence, the whole device cost and conduction loss can be reduced significantly compared to the structure proposed in [19] and [20]. The main metal oxide varistor (MOV2) undertaken the most of the energy absorption and withstand voltage. Another metal oxide varistors (MOV1) is used to protect the IGBT in LCS.

B. Operation Principles

In normal state that there is no fault, thyristor group (T1–T4) and IGBT (LCS) are turned ON, the normal current flows through the T1-LCS-T4 or T2-LCS-T3, as shown in Fig. 5(a). Since the current in both directions has the same operation principles due to the symmetrical structure, the unidirectional current of proposed solution is taken as an example in this section to explain the basic fault blocking principle.

1) *Step 1:* When the fault occurs, the fault current increases rapidly. As soon as the fault is detected, the LCS is turned OFF immediately and the fault current (I_{sys}) will be transferred from NCP to CCP to charge the capacitor C0, thus causing the current flows through thyristor group drop to zero, and forcing the thyristors to exit latch-up mode. During the charging process, the voltage of capacitor will continue to increase, creating a leakage current (I_{leak}) through MOV1, as shown in Fig. 5(b).
2) *Step2:* Because I_{leak} is less than the thyristor latching current, once the charging time from zero to clamping voltage of MOV1 is longer than the thyristor's maximum required turn-OFF time in datasheet (t_q), the thyristor group will be recovered in this stage under quasi-zero voltage, same as the solutions in [19], as shown in Fig. 5(c). In order to ensure the reliable turn OFF of thyristor, sufficient margin shall be reserved for capacitance value.
3) *Step 3:* After the thyristor is successfully turned OFF, the capacitor will be continuously charged to the clamping voltage of MOV2 (V_{clamp2}) and the fault current will be transferred to the energy absorption path, as shown in Fig. 5(d). Finally, the residual energy of the system inductor is absorbed by MOV2, and the fault current is reduced to zero.

III. Design Consideration

In order to ensure the success of fault blocking process, the key parameters such as commutating capacitor, MOV must be designed, and the electrical stress of semiconductor should be considered.

A. Commutating Capacitor

The most important issue of the fault blocking process for the proposed FB-MSSCB is to make sure that the recovery duration of the thyristors is longer than the intrinsic recovery time of the thyristor. The recovery duration depends on the charging process of capacitor until the capacitor's voltage V_c is larger than V_{clamp1}. Ignoring the leakage current of MOV1(I_{leak}), and considering the maximum blocking fault current ($I_{\max}$), the recovery duration T_{OFF} can be approximately expressed as

$$t_{\text{off}} = \frac{CV_{\text{clamp1}}}{I_{\max}} \geq t_q. \tag{1}$$

The capacitor C_0 can be chosen as

$$C \geq \frac{\alpha t_q I_{\max}}{V_{\text{clamp1}}} \tag{2}$$

where α is a redundancy factor, in order to ensure the reliable turn OFF of thyristor, 1.5–2 is suggested. For MVdc system, the volume of the capacitor becomes an important consideration in the design. It is estimated that the volume of capacitance is close to that of power electronic device valve bank.

B. Metal Oxide Varistor

As described in Section II, the parameters of two MOVs are different. The clamping voltage of MOVs can be expressed as

$$\begin{cases} V_{\text{clamp1}} = V_{\text{IGBT}}/\beta_1 \\ V_{\text{clamp2}} = \beta_2 \cdot V_{sys} \end{cases} \tag{3}$$

where V_{IGBT} is the maximum collector-emitter voltage of the IGBT, β_1 and β_2 are the redundancy factor, which are generally larger than 1. And V_{clamp2} is usually set higher than the system voltage (such as 1.5–2.5 times according to [21])

The main role of MOV1 is to protect the IGBT in LCS from overvoltage breakdown during the current commutating process, and the MOV1 design can refer to [22].

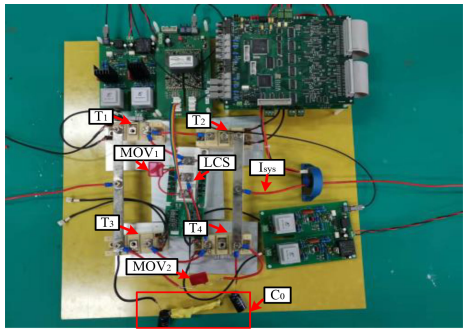

Fig. 6. Measured fault-interrupting waveforms of the FB-MSSCB.

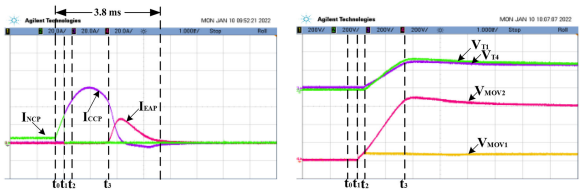

Fig. 7. Measured fault-interrupting waveforms of the FB-MSSCB. (a) Current curve of the experiment. (b) Voltage curve of the experiment.

For MOV2, a redesigned centralized MOV for MVdc or HVdc is required. In fact, similar centralized MOV have been applied in the HCBs of several VSC-HVdc projects [23].

C. Electrical Stress of Semiconductor Devices

The voltage electrical stress of semiconductor devices is limited by MOVs as mentioned previously, and the same as solutions in [19] and [20], the thyristor branches take most of system voltage, the maximum forward voltage stress of these thyristor branches can be expressed as

$$V_{Ti(i\,=\,1,2,3,4)} = \frac{V_{\text{clamp2}} - V_{\text{clamp1}}}{2}. \tag{4}$$

The current electrical stress of semiconductor devices depends on the current value at IGBT switching time, which is much smaller than the maximum fault current.

IV. Verification

A. Experimental Results

In this section, a scaled-down experimental prototype is built to verify the validity and feasibility of the proposed FB-MSSCB, as shown in Fig. 6. In the experiment, dc voltage is set to 500 V and system load current is about 5 A. In order to distinguish the different two MOV, V_{clamp1} of MOV1 is selected as 45V, and V_{clamp2} of MOV1 is selected as 600 V. The maximum fault current is about 60 A. The turn OFF time (t_q) of the selected thyristor is 150 μs, thus, the commutating capacitor's value is selected as 170 μF according to (4).

The fault current blocking process can be seen from Fig. 7, when the fault occurs at t_0, the system current [I_{NCP} in Fig. 7(a)] increases immediately, after 0.3 ms, the fault is detected and IGBT is turned OFF at t_1, the current is transferred from NCP to CCP and start charging the capacitor C_0 [I_{CCP} in Fig. 7(a)]. At this stage, the voltage of MOV1 increases with the capacitor voltage [V_{MOV1} in Fig. 7(b)], and is clamped at 45 V(V_{clamp1}) after the capacitor voltage (V_{C0}) reaches the clamping voltage of MOV1 at time t_2

The capacitor is continuously charged after t_2, and the voltage of MOV2 also rises [V_{MOV2} in Fig. 7(b)]. The time interval from t_1 to t_2 is more than 150 μs, which is greater than the maximum turn-OFF time of thyristor (t_q). Therefore, the thyristor can be successfully turned OFF. and thyristor branches T1 and T4 begin to share the difference between the capacitance voltage and V_{clamp1} [V_{T1} and V_{T4} in Fig. 7(b)]. At t_3, V_{C0} reaches the clamping voltage of MOV2 (V_{clamp2}), the fault current is transferred to EAP [I_{EAP} in Fig. 7(a)] and finally attenuates to zero.

TABLE II
Parameters of 10 kV/1 kA FB-MSSCB

Parameters	Value
Number of 4.5 kV IGBT	1
Number of 5.2 kV thyristor	8
Clamping voltage of MOV1	3 kV
Absorbing voltage of MOV1	1.5 kJ
Clamping voltage of MOV2	15k V
Absorbing voltage of MOV2	110.25 kJ
Capacitor voltage	18k V
Capacitor capacitance	3 mF
Capacitor Volume	75 cm*85 cm*40 cm

B. Engineering Application Example

In order to prove the potential of the proposed FB-MSSCB in practical engineering applications, according to Fig. 3, a 10 kV/1 kA FB-MSSCB model has been designed. The parameters of the 10 kV/1 kA FB-MSSCB are shown in Table II.

C. Comparative Analysis

In order to compare the improvements of the proposed structure in key characteristics more directly, the designed 10-kV/1-kAFB-MSSCB is compared with the bidirectional mixture-device based topology proposed by [19] and [20], one thyristor based SSCB proposed in [24], the bidirectional IGCT-based SSCB, and the bidirectional IGBT-based SSCB in the same power level. 4.5 kV IGBT(5SNA1200G452300), 5.2 kV thyristor(T1451N), 4.5 kV IGCT(5SHY35L4510) are selected in the comparison.

The relative conduction losses and costs are shown in Fig. 8. The calculation of costs in Fig. 8 only takes the capacitors, and semiconductor devices into consideration. The ordinate is a relative value and "1" means the maximum value, obviously, if the cost change of cooling system caused by the difference of conduction loss is taken into account, the proposed FB-MSSCB has significant advantages in both conduction losses and costs, it can achieve the lowest losses with less than half of the maximum costs. Furthermore, according to the characteristics of mixture device, with the increase of voltage level, the benefits of

TABLE III
COMPARISON WITH OTHER THYRISTOR-BASED BIDIRECTIONAL DC CIRCUIT BREAKERS

	Solution in [3]	Solution in [4]	Typical Z-source SSCB	Solution in [20]	Solution in [19]	Proposed Solution
Additional capacitor charging circuit or strategies	Yes	Yes	Yes	No	No	No
Negative overvoltage problem caused by reverse recovery process (RRP)	Yes	Yes	Yes	Yes	No	No
Blocking capability affected by outer circuit parameters	No	No	Yes	No	No	No

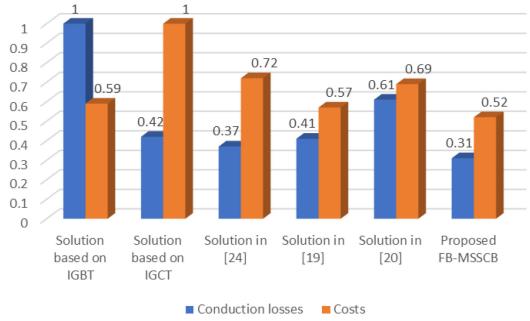

Fig. 8. Key characteristics comparison of six 10 kV/1 kA SSCB.

proposed FB-MSSCB will be more prominent when considering conduction losses and costs together.

The abovementioned comparison mainly selects several topologies with active blocking capability and the blocking capability is not affected by outer circuit parameters for comparison. Although the conduction loss of a few thyristor-based bidirectional SSCBs is lower than that of the topology proposed in this letter, there are some other problems, such as blocking capability affected by outer circuit parameters, additional capacitor charging circuit, several key features of six thyristor-based SSCBs are compared and summarized in Table III.

V. CONCLUSION

A novel FB-MSSCB topology combined with SCR and IGBT is proposed. Four thyristor branches and one fully-controlled device form a bridge structure. Compared with the existing mixture device based solid state circuit breaker topologies, only one fully controlled device is needed to realize bidirectional blocking, while the required number of thyristors remains unchanged, the device cost and conduction loss are significantly reduced. Experiments and comparative analysis verify the effectiveness and feasibility of the proposed topology.

REFERENCES

[1] Z. Shuai *et al.*, "Microgrid stability: Classification and a review," *Renewable Sustain. Energy Rev.*, vol. 58, pp. 167–179, May 2016.
[2] T. An, G. Tang, and W. Wang, "Research and application on multi-terminal and DC grids based on VSC-HVDC technology in China," *High Voltage*, vol. 2, no. 1, pp. 1–10, Mar. 2017.
[3] Z. Ayubu, J.-Y. Kim, J.-Y. Yu, S.-M. Song, and I.-D. Kim, "Novel bidirectional DC solid-state circuit breaker with operating duty capability," *IEEE Trans. Ind. Electron.*, vol. 68, no. 10, pp. 9104–9113, Oct. 2021.
[4] J. Shu, J. Ma, S. Wang, Y. Dong, T. Liu, and Z. He, "A new active thyristor-based DCCB with reliable opening process," *IEEE Trans. Power Electron.*, vol. 36, no. 4, pp. 3617–3621, Apr. 2021.
[5] R. Rodrigues, Y. Du, A. Antoniazzi, and P. Cairoli, "A review of solid-state circuit breakers," *IEEE Trans. Power Electron.*, vol. 36, no. 1, pp. 364–377, Jan. 2021.
[6] R. Wang, B. Zhang, S. Zhao, L. Liang, and Y. Chen, "Design of an IGBT-series-based solid-state circuit breaker for battery energy storage system terminal in solid-state transformer," in *Proc. 45th Annu. Conf. IEEE Ind. Electron. Soc.*, Oct. 2019, pp. 6677–6682.
[7] M. Kempkes, I. Roth, and M. Gaudreau, "Solid-state circuit breakers for medium voltage DC power," in *Proc. Electric Ship Technol. Symp.*, Apr. 2011, pp. 254–257, doi: 10.1109/ESTS.2011.5770877.
[8] Z. J. Shen, G. Sabui, Z. Miao, and Z. Shuai, "Wide-bandgap solid-state circuit breakers for DC power systems: Device and circuit considerations," *IEEE Trans. Electron Devices*, vol. 62, no. 2, pp. 294–300, Feb. 2015.
[9] J. Liu *et al.*, "Ultra-Low ON-State voltage IGCT for solid-state DC circuit breaker with single-switching attribute," *IEEE Trans. Power Electron.*, vol. 36, no. 3,pp. 3292–3303, Mar. 2021.
[10] C. Meyer and R. W. De Doncker, "Solid-state circuit breaker based on active thyristor topologies," *IEEE Trans. Power Electron.*, vol. 21, no. 2, pp. 450–458, Mar. 2006.
[11] Y. Guo, G. Wang, D. Zeng, H. Li, and H. Chao, "A thyristor full-bridge based DC circuit breaker," *IEEE Trans. Power Electron.*, vol. 35, no. 1, pp. 1111–1123, Jan. 2020.
[12] D. Keshavarzi, E. Farjah, and T. Ghanbari, "Hybrid DC circuit breaker and fault current limiter with optional interruption capability," *IEEE Trans. Power Electron.*, vol. 33, no. 3, pp. 2330–2338, Mar. 2018.
[13] R. Sander, M. Suriyah, and T. Leibfried, "Characterization of a countercurrent injection based HVDC circuit breaker," *IEEE Trans. Power Electron.*, vol. 33, no. 4, pp. 2948–2956, Apr. 2018.
[14] X. Diao, F. Liu, Y. Song, M. Xu, Y. Zhuang, and X. Zha, "Topology simplification and parameter design of Z/T/Γ source circuit breakers," *IEEE J. Emerg. Sel. Topics Power Electron.*, vol. 9, no. 6, pp. 7066–7077, Dec. 2021.
[15] Y. Yang and C. Huang, "A low-loss Z-source circuit breaker for LVDC systems," *IEEE J. Emerg. Sel. Topics Power Electron.*, vol. 9, no. 3, pp. 2518–2528, Jun. 2021.
[16] Z. Zhou, J. Jiang, S. Ye, C. Liu, and D. Zhang, "A Γ-source circuit breaker for DC microgrid protection," *IEEE Trans. Ind. Electron.*, vol. 68, no. 3, pp. 2310–2320, Mar. 2021.
[17] W. Li, Y. Wang, X. Wu, and X. Zhang, "A novel solid-state circuit breaker for on-board dc microgrid system," *IEEE Trans. Ind. Electron.*, vol. 66, no. 7, pp. 5715–5723, Jul. 2019.
[18] Y. Wang, R. Dong, Z. Xu, Z. Kang, W. Yao, and W. Li, "A coupled-inductor-based bidirectional circuit breaker for DC microgrid," *IEEE J. Emerg. Sel. Topics Power Electron.*, vol. 9, no. 3, pp. 2489–2499, Jun. 2021.
[19] X. Xu, W. Chen, C. Liu, R. Sun, Z. Li, and B. Zhang, "An efficient and reliable solid-state circuit breaker based on mixture device," *IEEE Trans. Power Electron.*, vol. 36, no. 9, pp. 9767–9771, Sep. 2021.
[20] J. Shu, S. Wang, J. Ma, T. Liu, and Z. He, "An active Z-source DC circuit breaker combined with SCR and IGBT," *IEEE Trans. Power Electron.*, vol. 35, no. 10, pp. 10003–10007, Oct. 2020.
[21] F. Liu, W. Liu, X. Zha, H. Yang, and K. Feng, "Solid-state circuit breaker snubber design for transient overvoltage suppression at bus fault interruption in low-voltage DC microgrid," *IEEE Trans. Power Electron.*, vol. 32, no. 4, pp. 3007–3021, Apr. 2017.
[22] L. Feng *et al.*, "Research on the breaking branch for a hybrid DC circuit breaker in ±500 kV voltage-sourced converter high-voltage direct current grid," *IET Power Electron*, vol. 13, no. 16, pp. 3560–3570, Dec. 2021.
[23] X. Zhang *et al.*, "A state-of-the-art_500 kV hybrid circuit breaker for a dc grid: The worlds largest capacity high-voltage dc circuit breaker," *IEEE Ind. Electron. Mag.*, vol. 14, no. 2, pp. 15–27, Jun. 2020.
[24] X. Xu *et al.*, "A novel thyristor-based bidirectional SSCB with controllable current breaking capability," *IEEE Trans. Power Electron.*, vol. 37, no. 4, pp. 4526–4534, Apr. 2022.